J. Chem. Sci. Vol. 129, No. 6, June 2017, pp. 721–731. © Indian Academy of Sciences.
DOI 10.1007/s12039-017-1278-2

REGULAR ARTICLE

Synthesis, characterization, X-ray structure, optical properties and theoretical calculations of condensed phthalazines

ESMA LAMERA[a], LYAMINE MESSAADIA[b], SOFIANE BOUACIDA[a,c], AISSA CHIBANI[a], KARIM BOUCHOUIT[d], BOUCHTA SAHRAOUI[e] and ABDELMALEK BOURAIOU[a,*]

[a]Unité de Recherche de Chimie de l'Environnement et Moléculaire Structurale, Université des Frères Mentouri, Constantine 25000, Algeria
[b]Laboratoire Énergétique Appliquée et Matériaux, Université de Jijel, 18000 Jijel, Algeria
[c]Département des sciences de la matière, Université Oum El Bouaghi, 04000 Oum El Bouaghi, Algeria
[d]Ecole Normal Supérieure de Constantine, Ville Universitaire, Ain El Bey Ali Mendjeli, Constantine, Algeria
[e]CNRS UMR 6200, Laboratoire MOLTECH-Anjou, LUNAM Université, Université d'Angers, 2 Bd Lavoisier, 49045 Angers Cedex, France
E-mail: bouraiou.abdelmalek@yahoo.fr

MS received 5 February 2017; revised 6 April 2017; accepted 10 April 2017

Abstract. Two condensed phthalazine compounds were synthesized and characterized by FT-IR, UV-Vis, NMR spectroscopic studies. Single crystal XRD and molecular orbital calculations. Optimized geometrical structures were computed with RB3LYP method with the 6-31G(p, d) basis set. The geometrical parameters of both compounds obtained from Single Crystal XRD were found to be in accord with the calculated (DFT) values. The electronic contribution $\chi_{THG}^{<3>}$ was measured using the third harmonic generation technique on thin films at 1064 nm for both compounds. Also, the values of dipole moment μ, the average polarizability $\bar{\alpha}$, and the first static hyperpolarizability (β_0) were computed. The theoretical and experimental results confirm the NLO behavior of both compounds.

Keywords. Condensed phthalazine; DFT calculations; spectroscopic analysis; X-ray structure; NLO.

1. Introduction

Phthalazine belongs to the azine class of molecules. It is an important group of heterocyclic compound which contains bridgehead hydrazine in a fused ring system and has a wide range of pharmaceutical and biological activities such as antitumor,[1] antimicrobial,[2] antifungal,[3] anti-inflammatory,[4] antioxidant activities[5] and vasorelexant effect.[6] In addition, these compounds are promising materials for the development of new luminescent materials and fluorescence probes.[7]

Organic molecular systems having an electron donor and electron acceptor group linked through a π - conjugated electronic bridge are of great interest because of their application as potential materials in modern chemistry and material science.[8–10] The dipolar type, with a donor–bridge–acceptor (D-π-A) motif, plays a vital role in NLO activity. The design of new push-pull π-conjugated molecular system with strong NLO response was developed by many researchers, based on intramolecular charge transfer through a π- conjugated framework from a good electron donor to a good electron acceptor group which will improve the NLO susceptibility.[11]

In the present work, based on the above considerations and in continuation of our research in NLO field,[12,13] two condensed phthalazines containing push-pull π-conjugated system were synthesized. In these molecules, the amine or methyl group acts as electron-donor and the nitrile or carbonyl group acts as the electron-acceptor. The spectroscopic characterization and crystal structure are reported. Third-order NLO properties were measured using the third harmonic generation technique on thin films at 1064 nm. The quantum chemical parameters, such as E_{HOMO}, E_{LUMO}, ΔE, dipole moment (μ), average polarizability and first hyperpolarizability were calculated using Density Functional Theory (DFT). The relationship between structure of compounds and their properties were investigated both experimentally and theoretically.

*For correspondence

2. Experimental

2.1 *General considerations*

All the chemicals used were of the analytical reagent grade and were used as received. ^{1}H-NMR and ^{13}C-NMR measurements were recorded at room temperature on a Brüker Avance DPX250 and Brüker Avance 300 spectrometers. The melting point was determined using an Electrothermal IA9100 digital melting point apparatus. UV/Vis spectrum of the compound was recorded in the region of 200–600 nm using an Optizen 1220 UV/Vis Spectrophotometer. Fourier transform-infrared (FT-IR) measurements were carried out by the KBr method using a Shimadzu FT/IR-8201 PC spectrophotometer.

2.2 *Synthesis*

2.2a *Synthesis of 3-amino-5,10-dioxo-1-(p-tolyl)-5,10-dihydro-1H-pyrazolo[1,2-b]phthalazine-2-carbonitrile (**1**)*: Compound **1** was synthesized following a literature procedure starting from a mixture of phthalhydrazide (1.0 mmol), *p*-tolualdehyde (1.1 mmol), malononitrile 4 (1.05 mmol) and Et_3N (20% mol) in ethanol.[14] Yield 80%; yellow solid; M.p. 261–262°C (lit. = 253–255°C[15]); IR (KBr) ν /cm^{-1}: 3359, 3259, 3039, 2194, 1658, 1569, 1434, 1380, 1276, 1149, 1026, 694, 574; ^{1}H NMR (300 MHz, DMSO-d_6): δ : 8.26–8.25 (m, 1H), 8.11–8.09 (m, 3H), 8.00–7.96 (m, 2H), 7.35 (d, 2H, J = 7.9 Hz), 7.18 (d, 2H, J = 7.9 Hz), 6.10 (s, 1H), 2.31 (s, 3H) ppm; ^{13}C NMR (75 MHz, DMSO-d_6): δ : 157.0 (C), 154.0 (C), 151.0 (C), 138.1 (C), 135.9 (C), 135.1 (CH), 134.1 (CH), 129.5 (CH), 129.2 (C), 129.1 (C), 127.7 (CH), 127.3 (CH), 127.1 (CH), 116.5 (C), 63.3 (CH), 61.9 (C), 21.2 (CH_3) ppm; UV–Vis (MeOH, λ /nm): 220, 240, 355.

2.2b *Synthesis of 13-(p-tolyl)-2,3,4,13-tetrahydro-1H-indazolo[1,2-b]phthalazine-1,6,11-trione (**2**)*: Compound **2** was synthesized following a literature procedure starting from a mixture of phthalhydrazide (1.0 mmol), *p*-tolualdehyde (1.1 mmol), cyclohexane-1,3-dione (1.05 mmol) and H_2SO_4 (15% mol) in EtOH-H_2O.[16] Yield 83%; yellow solid; M.p. 247–249°C (lit. = 245–246°C[17]; IR (KBr) ν /cm^{-1}: 3460, 3028, 2939, 1658, 1512, 1465, 1419, 1103, 995, 783, 698, 532 cm^{-1}; ^{1}H NMR (250 MHz, $CDCl_3$): δ : 8.30–8.25 (m, 1H), 8.13-8.08 (m, 1H), 7.98–7.92 (m, 2H), 7.32 (d, 2H, J = 8.0 Hz,), 7.11 (d, 2H, J = 7.8 Hz), 6.27 (s, 1H), 3.49–3.18 (m, 2H), 2.53–2.34 (m, 2H), 2.32 (s, 3H), 2.17–2.11 (m, 2H) ppm; ^{13}C NMR (62.9 MHz, $CDCl_3$): δ : 192.8 (C), 155.7 (C), 154.0 (C), 153.3 (C), 137.7 (C), 135.0 (CH), 134.9 (C), 134.1 (CH), 129.4 (C), 129.2 (CH), 129.1 (C), 128.0 (CH), 127.8 (CH), 127.2 (CH), 118.9 (C), 64.6 (CH), 36.9 (CH_2), 24.4 (CH_2), 22.3 (CH_2), 21.1 (CH_3) ppm; UV–Vis (MeOH, λ /nm): 220, 245, 276, 360.

2.3 *X-ray crystallography*

Single Crystal XRD data were collected on a Bruker Apex II diffractometer. All diffraction measurements were performed at 273 K using graphite monochromated Mo-Kα radiation (λ = 0.71073Å). The structures were solved by direct methods with SIR2002[18] to locate all the non-H atoms which were refined anisotropically with SHELXL97.[19,20] All absorption corrections were performed with the SADABS program.[21] All the H atoms were placed in the calculated positions and constrained to ride on their parent atoms.

2.4 *Nonlinear optical properties*

2.4a *Preparation of thin films*: Compounds **1** and **2** were dissolved in chloroform (5 mg/mL). The films were deposited by spin coating technique on BK7 glass substrates with an angular speed of 600–1000 rpm. After the deposition, the thin films of the studied compounds were dried in an oven at 60°C for 20 min in order to eliminate any remaining solvent. The thickness of the layers was around 100 nm, as measured with a 6M DEKTAK profile-meter.

2.4b *THG measurement*: The electronic contribution $\chi_{THG}^{<3>}$ values of the compounds **1** and **2** was evaluated by using the third harmonic generation (THG) method on thin films at 1064 nm. Third harmonic (TH) signal was analyzed with fused silica as reference material using the Maker fringes technique.[22] More details of the experimental setup were reported in our previous works.[12,13]

2.5 *Computational studies*

The optimized geometrical parameters were calculated using the Gaussian 09 package[23] and the Gauss-View molecular visualization program.[24] Stationary points have been positively identified for local minima with the number imaginary frequencies (NIMAG=0). Density functional theoretical (DFT) methods used the combination of the Becke exchange functional RB3LYP[25] combined with the 6-31G(p, d) basis set. The quantum chemical parameters, such as E_{HOMO}, E_{LUMO}, ΔE (energy gap), dipole moment (μ), average polarizability, and first static hyperpolarizability were calculated.

3. Results and Discussion

3.1 *Synthesis*

The routes to the target compounds **1** and **2** are shown in Scheme 1. Compound **1** was obtained *via* the multicomponent reaction under ultrasonic irradiation of phthalhydrazide (1 mmol), 1.05 mmol of malononitrile and 1.05 mmol of *p*-tolualdehyde using triethylamine (Et_3N) as catalyst in ethanol. The result is excellent in terms of yield and product purity. Compound **2** was obtained in a one-pot mutlicomponent reaction of 1 mmol of phthalhydrazide, 1 mmol of cyclohexane-1,3-dione and 1.05 mmol of *p*-tolualdehyde employing a

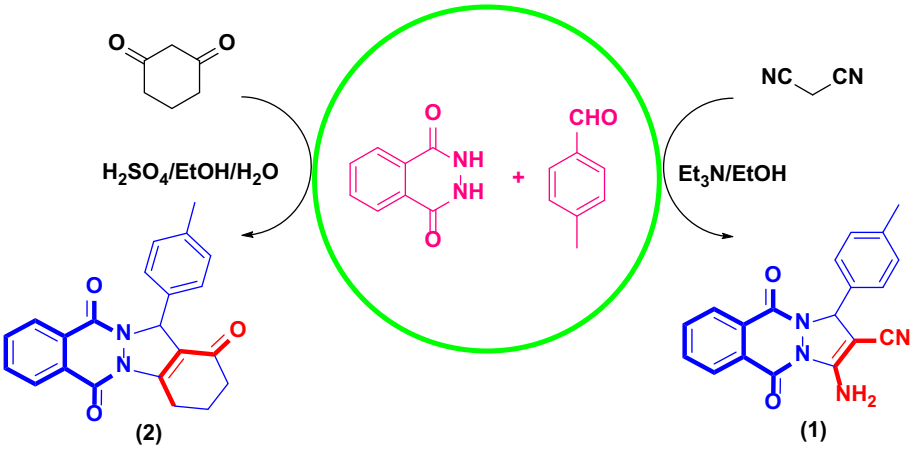

Scheme 1. Synthesis of compounds **1** and **2**.

mixture of EtOH-H_2O as solvents and catalytic quantity of sulfuric acid. Two hours are sufficient for complete conversion of the starting materials. The crude product was isolated in good yield and no further purification process was required.

The identity of both known compounds was confirmed by comparison of their melting points and spectral data (UV, IR, ^{1}H and ^{13}C NMR) with those reported in the literature. The ^{1}H NMR spectrum of compound **1** shows one multiplet between 8.11 and 8.09 ppm due to the –NH_2 of the pyrazole ring and one aromatic proton. The signals phthalazine protons are found at intervals [8.26–8.25] and [8.00–7.96] ppm as multiplets. The signals of the aromatic protons of the tolyl group appear at 7.35 and 7.18 ppm as doublets (J = 7.9 Hz). The signal attributable to the proton of the pyrazole ring is found at 6.10 ppm as singlet. The ^{13}C NMR spectrum data in **1** showed the signals of the two C=O carbon at 157.0 and 154.0 ppm. The carbon of the pyrazolo ring is observed at 63.3 ppm. The signal attributable to the carbon of the nitrile is found at 61.9 ppm. The signals of other aromatic carbons appear between 151.0 and 116.5 ppm. The observed in FT-IR band at 2194 cm^{-1} is due to C≡N stretching vibration. The ^{1}H NMR spectrum of **2** shows signals of the aromatic protons between 8.30 and 7.11 ppm as multiplets. The singlet at 6.27 ppm is due to the proton of the pyrazole ring. The signals of the methylene protons are found between 3.49 and 2.11 ppm as multiplets. The ^{13}C NMR spectrum data in compound **2** showed the signals of the three C=O carbons at 192.8, 155.7 and 154.0 ppm. The carbon signal of the pyrazolo ring is at 64.6 ppm. The signals of the aromatic carbons appear between 153.3 and 118.9 ppm. The signals the methylene carbons appear at 36.9, 24.4 and 22.3 ppm. The characteristic FT-IR band appearing at 1658 cm^{-1} in the **2** confirms the presence of carbonyl group.

3.2 *Crystal structures*

Both the compounds were recrystallized and suitable crystals of **1** and **2** were grown in DMF and $CHCl_3$/Dioxane solutions, respectively. The X-ray crystallographic analysis confirmed their respective structures and the refined X-ray crystal structures are shown in Figures 1 and 2. Crystal data, structure refinement parameters, selected angles, bond lengths and some intra- and intermolecular interactions hydrogen bonds for compounds **1** and **2** are listed in Tables 1, 2 and 4.

3.2a *Crystal structure of compound **1***: Compound **1** crystallizes in tetragonal system with $I4_1/a$ space group (Z = 16). The asymmetric unit consists of one enantiomer with absolute stereochemistry R of the stereogenic centre C9. However, the second one is generated by a crystallographic inversion centre. The structure of **1** is composed of phthalazine ring fused to pyrazolo moiety and one phenyl group attached. The pyrazole ring is planar and forms dihedral angle of 86.96(8)° with the tolyl group. The bond distances C9–N2 and C11–N1 are 1.483(2) Å and 1.405 (2) Å, respectively, while the distance C12–N4 is 1.152(3) Å (Table 4). The carbonyl bond lengths C8–O2 (1.231(2) Å), C1–O1 (1.230(2) Å) show a typical double bond character. The crystal packing can be described as double layers in zig-zag along the c axis (Figure 1). These layers are connected with N–H · · · O and N–H · · · N hydrogen bonds interactions (Table 2). The crystal structure is also supported by π − π stacking interactions.

3.2b *Crystal structure of compound **2***: Compound **2** crystallizes in the monoclinic space group P21/c with Z = 4 (Table 1). X-ray crystallography of compound **2** showed that the unit cell contains two pairs of

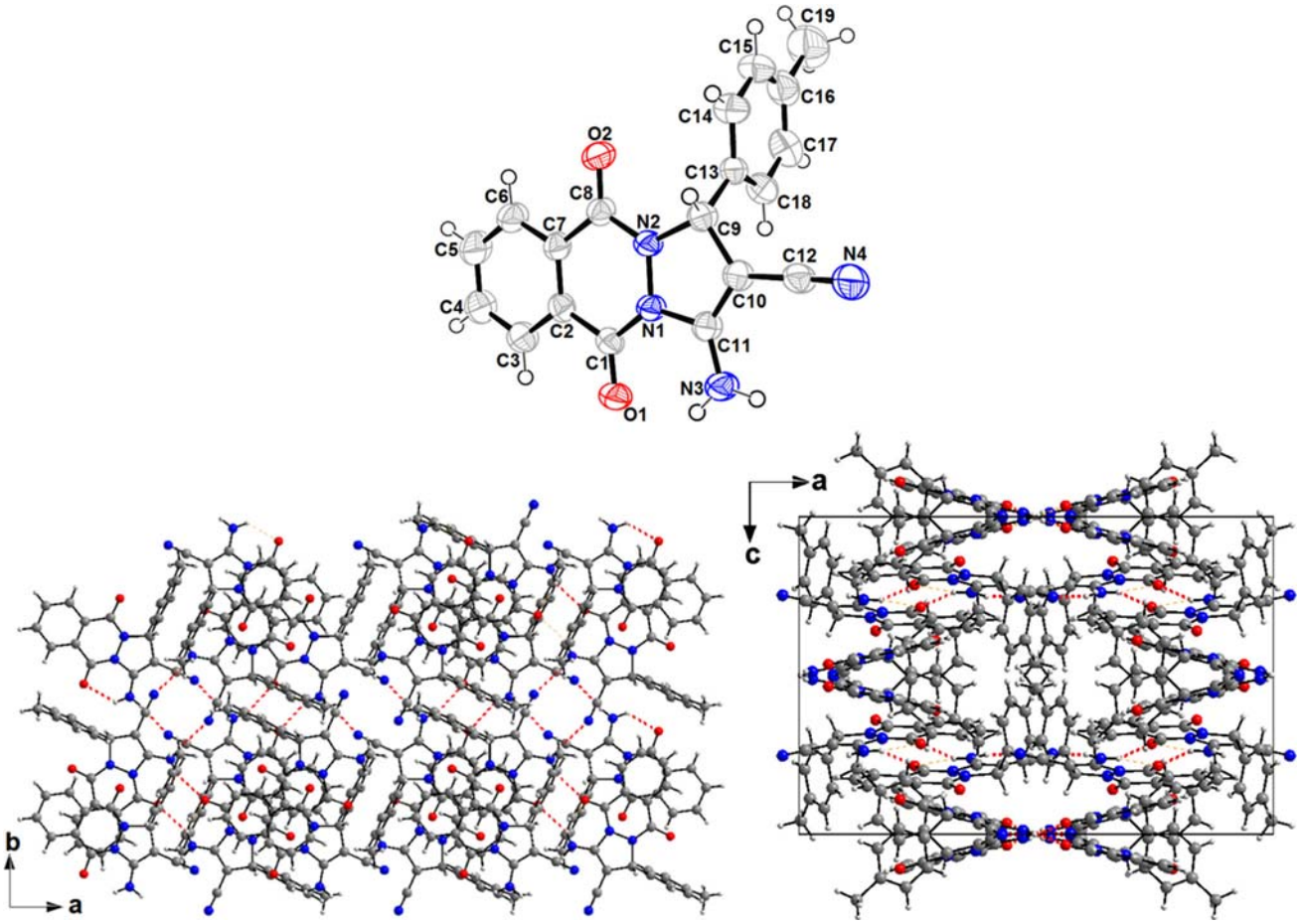

Figure 1. (*a*) The molecular structure of compound **1** showing the atom numbering scheme. Displacement ellipsoids are drawn at 50% probability level. (*b*) View of N–H · · · N and N–H · · · O interactions leading to supramolecular layers; (*c*) Crystal packing shows formation of layers in zig-zag along the c axis.

stereoisomers generated by a crystallographic inversion centre. The analysis shows that the two enantiomers have for each one, the absolute stereochemistry (*R*) and (*S*) of the new stereocenters created in the cyclocondensation reaction. The asymmetric unit consists of an indazolone moiety fused to a phthalazine ring system and bearing a tolyl group at the stereogenic centre C9 (Figure 2). The phenyl ring (C13-C18) is almost normal to the mean plane of the five-membered ring (N1/N2/C9–C11) of the indazolone moiety with a dihedral angle of 84.02(8)°. The cyclohexene ring (C10–C12/C20–C22) is fused to the pyrazolidine ring, so forming the indazolophthalazine unit, has a half-chair conformation with the central methylene C atom, C21, as the flap. The carbonyl bond lengths C8–O2 (1.221(2) Å), C1–O1 (1.221(2) Å) and C12–O3 (1.229(3) Å), show a typical double bond character. The C–N bonds, C1–N1 (1.382 (2) Å), C8–N2 (1.346(3) Å) and C11–N1 (1.385 (3) Å) indicate partial double bond character while the bond length, C9–N2 (1.473 (3) Å) shows single bond character. The crystal packing can be described by alternating layers parallel to (101) plane (Figure 1) and molecules are linked also *via* C–H · · · O intermolecular hydrogen bonds forming alternating layers parallel to (101) plane (Table 2 and Figure 2). Furthermore, the crystal packing is consolidated by π − π stacking interactions.

3.3 *Nonlinear optical properties*

Figure 3 shows the UV-Visible spectra of compounds **1** and **2** in methanolic solution. These spectra were recorded using a cuvette with a path length of 10 mm and concentration of 1.66×10^{-5} mol/L. From the spectra, we can observe that these molecules exhibit two absorption bonds with λ_{max} at ∼ 240 and ∼ 360 nm, which correspond to the π → π ∗ and n → π* transitions attributed to the different units of the molecule.

For the third order NLO susceptibility, SiO_2 was used as a standard reference material to calibrate THG measurements. Third order nonlinear optical susceptibility of SiO_2 was estimated to be $\chi^{<3>} = 2.00 \cdot 10^{-22} \left[m^2/V^2\right]$.[26] For the calculation of electronic

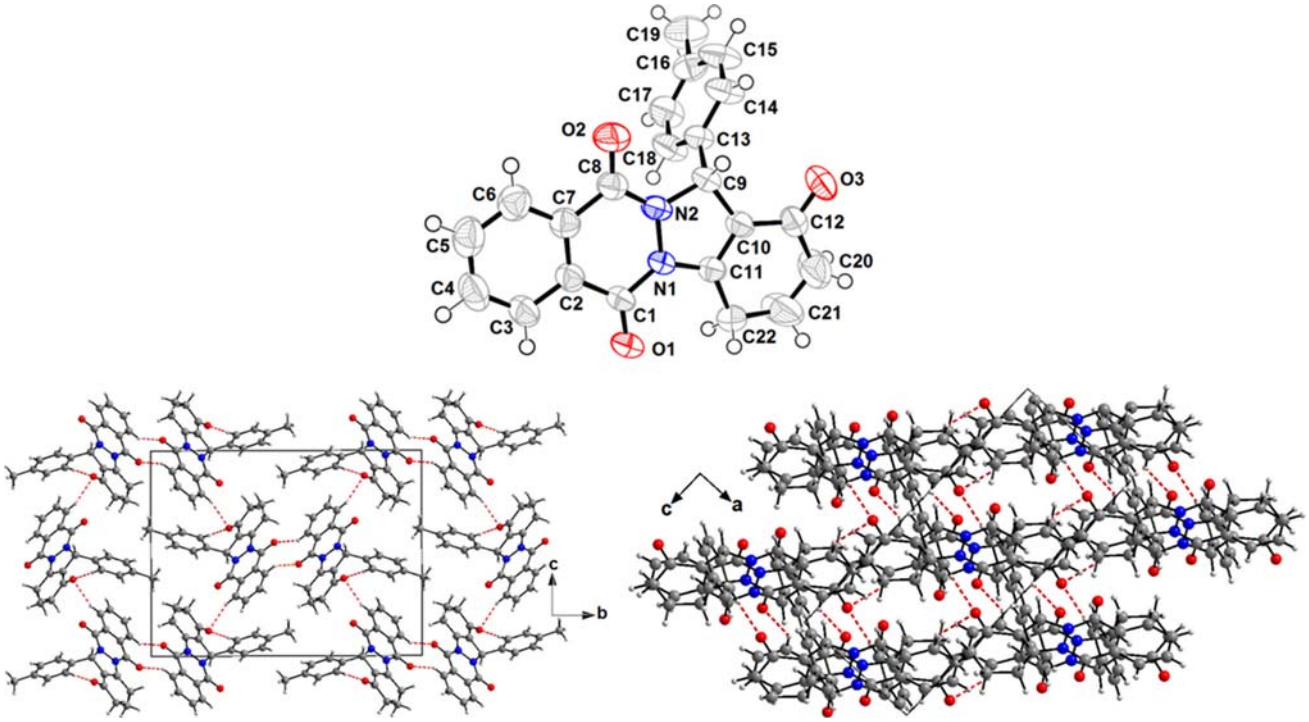

Figure 2. (*a*) The molecular structure of compound **2** showing the atom numbering scheme. Displacement ellipsoids are drawn at 50% probability level. (*b*) View of C–H · · · O interactions leading to supramolecular layers along the b axis; (*c*) Formation of alternating double layers parallel to (101).

contribution $\chi^{<3>}$ susceptibilities, we have used the model of Kubodera and Kobayashi:[27]

$$\chi^{(3)} = \chi^{(3)}_{silica} \frac{2}{\pi} \frac{l_{c,s}}{d} \sqrt{\frac{I^{3\omega}}{I^{3\omega}_{silica}}} \tag{1}$$

$$l_{c,s} = \frac{\lambda_\omega}{6(n_{s(3\omega)} - n_{s(\omega)})} \tag{2}$$

Here, $\chi^{<3>}$ and $\chi^{<3>}_{silica}$ are the third order nonlinear susceptibilities of the studied compounds and silica (SiO_2), respectively, $I^{3\omega}$ and $I^{3\omega}_s$ are the TH intensities of the compound studied and the standard reference (silica), respectively, d is thickness of film, λ_ω is the wavelength of the fundamental laser beam ($\lambda_\omega = 1064$ nm), and $n_{s(\omega)}$ and $n_{s(3\omega)}$ are the refractive indices of silica at the wavelength of the fundamental and the third harmonic beam, respectively ($n_{s(\omega)} = 1.4496$ at 1064 nm and $n_{s(3\omega)} = 1.4761$ at 355 nm). $l_{c.s}(1064\,\text{nm}) = 6.69\,\mu\text{m}$.

The TH intensity as a function of the incident angle presented in Figure 4 for compounds **1** and **2** shows that **1** presents a higher THG response compared to compound **2**. We have used eq. 1 for the calculation of $\chi^{<3>}_{THG}$ susceptibilities. The values obtained from THG measurements for compounds **1** and **2** are reported in Table 3.

The values of susceptibility $\chi^{<3>}_{THG}$ of compounds **1** and **2** as thin films at the measurement wavelength of 1064 nm are 0.46. $10^{-20}\left[m^2/V^2\right]$ and 0.30 $10^{-20}\left[m^2/V^2\right]$, respectively (Table 3). These values are one order of magnitude higher than that for SiO_2, which is the reference material. Also, we can observe from Table 3 that the $\chi^{<3>}_{THG}$ of compound **1** is higher than that of **2**, and this difference is due to their molecular structures. Compounds **1** and **2** have the same chemical nucleus; however, Compound **1** possesses a better electron-drawing group (–CN) and better electron-donating group ($-NH_2$), which favor greater charge transfer compared to compound **2**.

3.4 *Computational details*

3.4a *Geometrical structure*: The optimized structure parameters (bond lengths and angles) obtained using the RB3LYP/6-31G(d, p) basis set for the compounds **1** and **2** are compared with experimental data in Table 4. The geometry structures are followed by the vibrational analysis to check the absence of imaginary frequencies. The selected bond lengths and angles are in good agreement with their corresponding values deduced from X-ray diffraction. The small deviations are probably due to the intermolecular interactions in the compounds. Additionally, we note that the experimental results belong to the solid state and the theoretical calculations belong the gas phase.

Table 1. Crystallographic data and refinement parameters for compounds (**1**) and (**2**).

	Compound **1**	Compound **2**
Formula	$C_{19}H_{14}N_4O_2$	$C_{22}H_{18}N_2O_3$
Formula weight	330.34	358.38
Crystal habit, color	Prism, Colorless	Prism, Colorless
Crystal system	Tetragonal	monoclinic
Space group	$I4_1/a$	P21/c
a (Å)	21.4765(8)	6.2993(9)
b (Å)	21.4765(8)	19.436(3)
c (Å)	14.3538(6)	14.739(2)
α (°)	90	90
β (°)	90	91.626(7)
γ (°)	90	90
Volume (Å^3)	6620.5(4)	1803.8(4)
Z	16	4
Density (calculated, g cm^{-3})	1.326	1.32
Absorption coefficient (mm^{-1})	0.09	0.089
F(000)	2752	752
Crystal size (mm)	0.15 × 0.13 × 0.11	0.09 × 0.13 × 0.22
θ range for data collection (°)	3.14–24.32	3.47–32.49
Reflections collected	12818	20311
Independent reflections	3290	5349
R_{int}	0.0464	0.0407
Reflections with $I \geq 2\sigma(I)$	2034	3188
Number of parameters	227	239
Goodness-of-fit on F^2	1.017	1.033
Final R indices [$I \geq 2\sigma(I)$]	0.0482	0.0777
R indices [all data]	$R_1 = 0.0898$, $wR_2 = 0.1567$	$R_1 = 0.1249$, $wR_2 = 0.2137$
Largest difference peak and hole (Å^{-3})	0.187, −0.183	0.566, −0.415

Table 2. Distances (Å) and angles (°) of hydrogen bonds for compounds **1** and **2**.

D–H · · · A	*d*(D–H)	*d*(H · · · A)	*d*(D–A)	D–H–A	Symmetry
Compound **(1)**					
N3–H3A · · · N4	0.86	2.229	3.070(3)	166	−x + 2, −y + 1/2, z
N3–H3B · · · O1	0.86	2.088	2.713(3)	129	x, y, z
N3–H3B · · · O1	0.86	2.320	3.085(3)	148	−x + 2, −y, −z + 1
Compound **(2)**					
C3–H3 · · · O1	0.93	2.47	3.259(3)	142	2−x, −y, −z
C6–H6 · · · O3	0.93	2.40	3.193(3)	143	1+x, 1/2−y, −1/2 + z
C18–H18 · · · O3	0.93	2.44	3.368(3)	175	1+x, y, z

3.4b *Frontier molecular orbitals (HOMO–LUMO) analysis*: The frontier molecular orbital (FMOs) energies and the gap analysis are useful for understanding the chemical reactivity and optical properties of organic compounds. The important molecular orbitals in a compound are the highest occupied molecular orbital (HOMO) and lowest unoccupied molecular orbital (LUMO). The HOMO energy represents the ability to donate an electron and LUMO represents the ability to accept an electron. The energy gap of orbitals ($\Delta E_{H-L} = E_{HOMO} - E_{LUMO}$) was calculated at B3LYP/6-31G(p, d) level, which reveals the chemical reactivity of molecule and proves the occurrence of eventual charge transfer within molecule. The frontier orbital gap helps to characterize the chemical reactivity and kinetic stability of the molecule. A molecule with a small frontier orbital gap is more polarizable and is generally associated with a high chemical reactivity,

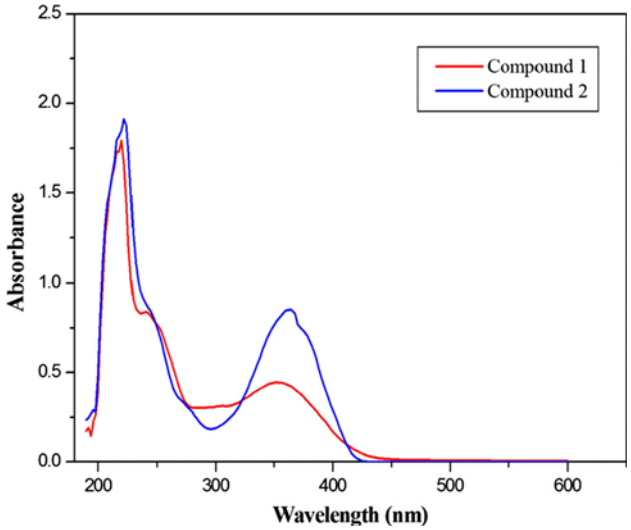

Figure 3. The absorption spectra of compounds **1** and **2**.

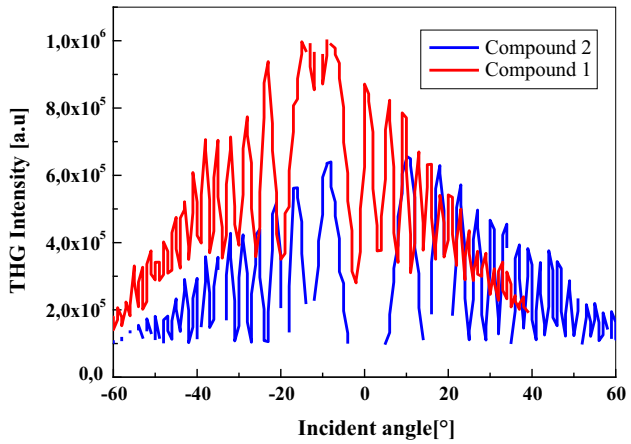

Figure 4. Third harmonic intensity as a function of the incident angle for compounds **1** and **2**.

Table 3. The values of third order nonlinear optical susceptibility ($\chi_{THG}^{<3>}$) for compounds **1** and **2** as thin films of thickness d, obtained from THG measurements.

	d (nm)	$\chi_{THG}^{<3>}.10^{22}\,[m^2/V^2]$
Compound **1**	160	46.4
Compound **2**	~100	29.65
Silica	–	2

low kinetic stability and is also termed as soft compound.[28] The calculated HOMO and LUMO gaps are presented in Table 5, the frontier orbital gaps ΔE (H-L) of compounds **1** and **2** are 3.692 and 3.812 eV, respectively. This result shows that compound **1** is slightly more reactive than **2**, and affirms the occurrence of eventual intermolecular charge transfer and delocalization of electron density within the compound **1**.

The 3D plots of the frontier molecular orbitals HOMO and LUMO, for the both compounds are shown in Figure 5. It can be seen that, the HOMO for the compounds **1** and **2** is localized over the C=O, N–N, NH_2 and CN atoms. The LUMO is almost distributed on the entire compound except the toluene ring.

3.4c *First hyperpolarizability*: All the quantum chemical calculations were performed using Density Functional Theory (DFT) using RB3LYP/6-31G(p,d) basis set. The polarizabilities and first static hyperpolarizability characterize the response of a system in an applied electric field.[29,30] The components of GAUSSIAN 09 output are reported in atomic units and therefore the calculated values are converted into electrostatic units (esu) (1 a.u = 8.36939×10^{-33} esu). The First hyperpolarizability is a third rank tensor that can be described by a $3 \times 3 \times 3$ matrix. The 27 Components of the 3D matrix can be reduced to 10 components due to the Kleinman symmetry.[31] The total dipole moment μ, the average polarizability $\bar{\alpha}$, and the first static hyperpolarizability (β_0), using the x, y, z components are defined as follows:

$$\mu = \left(\mu_x^2 + \mu_y^2 + \mu_z^2\right)^2 \tag{3}$$

$$\overline{\alpha} = \frac{\alpha_x + \alpha_x + \alpha_x}{3} \tag{4}$$

$$\beta_0 = \left(\beta_x^2 + \beta_y^2 + \beta_z^2\right)^{1/2} \tag{5}$$

where $\beta_x = \beta_{xxx} + \beta_{xyy} + \beta_{xzz}$, $\beta_y = \beta_{yyy} + \beta_{yzz} + \beta_{yxx}$ and $\beta_z = \beta_{zzz} + \beta_{zxx} + \beta_{zyy}$.

In order to study the correlation between the compound and Non-Linear Optical proprieties (NLO), the components of the polarizabilities, hyperpolarizabilities (β) and average polarizability α(Å^3) were calculated. The components of the first hyperpolarizability for the compounds **1** and **2** are listed in Table 6.

As seen, the first hyperpolarizability of compound **1** is 1.83 times greater than that of **2**. The results indicate that **1** is a better candidate for use as nonlinear optical material than **2**. It is expected that compound **1** has NH_2 as the donor group and CN as accepter group which increase of first hyperpolarizability when compared to compound **2** where $–CH_2–$ acts as donor and C=O as accepter group.

According to the present study, the calculated values of the dipole moment μ_{tot}, average polarizability $\bar{\alpha}$, and the first static hyperpolarizability (β_0) of compound **1** are equal to 5.253 Debye, 36.314 Å^3 and 1.209×10^{-29}esu, respectively (Table 7). In case of the compound **2**, these values are 3.477 Debye, 34.877 Å^3 and 6.58×10^{-30} esu, respectively. The calculated average polarizability $\bar{\alpha}$ and

Table 4. Selected bond lengths (Å) and angles (°) for compounds **1** and **2** with estimated standard deviations. Theoretical structure parameters obtained by RB3LYP/6-31G(p,d) are given in parentheses.

Bond lengths/bond angles	Compound **1**	Compound **2**
N1– N2	1.411(2)	1.417(2)
	(1.410)	(1.418)
C10– C11	1.357(3)	1.355(3)
	(1.370)	(1.355)
C9– C13	1.517(3)	1.514(3)
	(1.524)	(1.526)
C10– C12	1.403(3)	1.432(3)
	(1.405)	(1.459)
N1– C11	1.405(2)	1.385(3)
	(1.404)	(1.395)
N2– C9	1.483(2)	1.473(3)
	(1.486)	(1.478)
C8– O2	1.231(2)	1.221(2)
	(1.226)	(1.226)
C1– O1	1.230(2)	1.221(2)
	(1.235)	(1.226)
C12– N4	1.152(3)	–
	(1.168)	
C12– O3	–	1.229(3)
		(1.225)
N1– C1– O1	120.41(17)	120.6(2)
	(121.19)	(121.2)
N2– N1– C1	123.06(15)	107.61 (18)
	(123.99)	(107.69)
N1– N2– C9	111.63(14)	110.88(17)
	(111.15)	(110.80)
N2– C9– C10	99.20(14)	100.14(15)
	(100.06)	(99.99)
N1– C11– C10	109.22(17)	110.48(18)
	(109.78)	(109.99)

Table 5. Quantum chemical parameters of compounds **1** and **2** calculated by DFT using the RB3LYP/6-31G (d, p).

Parameters	Compound **1**	Compound **2**
Total energy (Hartree)	−1101.92426338	−1184.39767286
$E_{HOMO}(eV)$	−5.837	−5.964
$E_{LUMO}(eV)$	−2.145	−2.152
ΔE_{H-L}(eV)	3.692	3.812

dipole moment of compound **2** is about 1.041, 1.51 times, respectively, greater than those of **1**. In addition, these results prove that compound **1** shows better NLO behavior.

4. Conclusions

We have presented in this work the synthesis, structural characterization, nonlinear optical properties (NLO) and theoretical calculations for two condensed phthalazines. These compounds were obtained by a multicomponent reaction of *p*-tolualdehyde, phthalhydrazide and activated methylene. The structure of both compounds were established with usual spectroscopic methods and confirmed by X-ray analysis. Compound **1** shows better nonlinear optical effect than **2**. This is in good agreement with the results obtained from Density Functional Theory (DFT); therefore, charge transfer

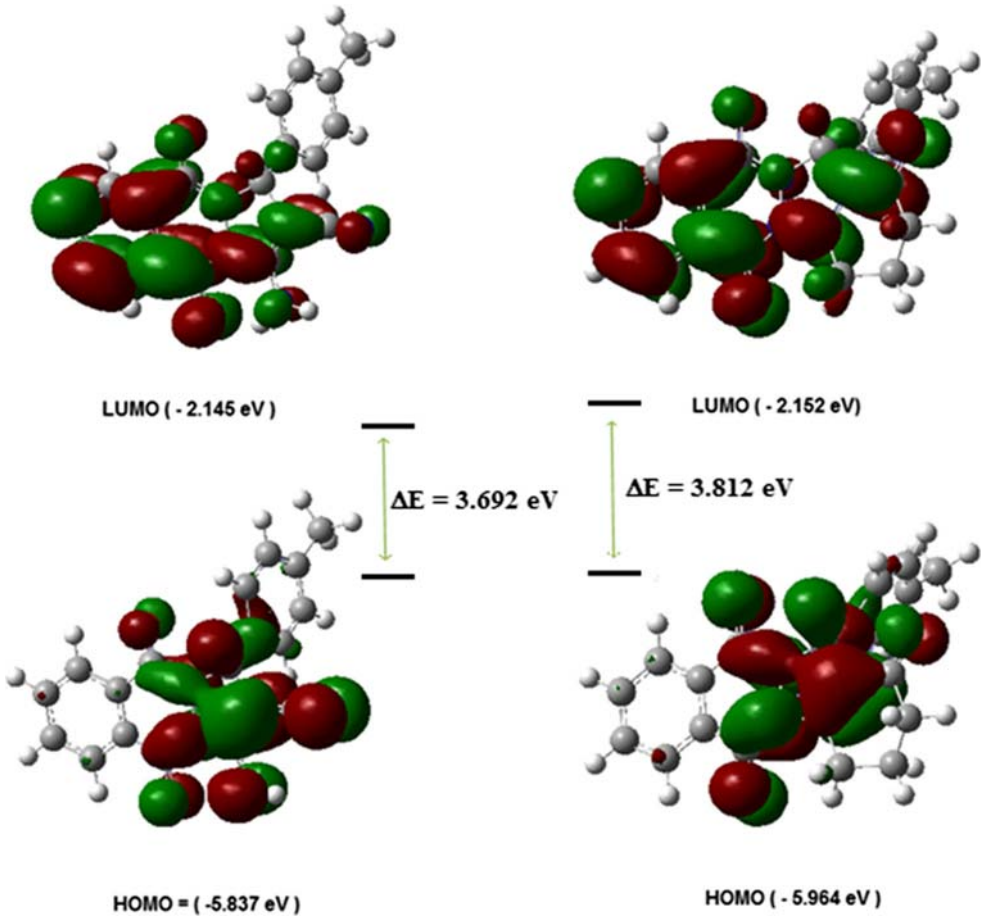

Figure 5. Frontier molecular orbitals of compounds **1** and **2**.

Table 6. Calculated β components and β_{tot}, using RB3LYP/6-31G(p, d) for compounds **1** and **2**.

Components	Compound **1**	Compound **2**
β_{xxx}	−0.135281	−0.632438
β_{xxy}	−0.200071	0.338251
β_{xyy}	0.404718	0.227007
β_{yyy}	0.740081	0.288506
β_{xxz}	−0.246261	0.816194
β_{xyz}	0.841411	−0.153842
β_{yyz}	−0.587429	−0.756012
β_{xzz}	−0.611213	−0.192385
β_{yzz}	−0.406538	0.165012
β_{zzz}	0.280832	0.367805
β_{tot} (esu)	1.209×10^{-29}	6.58×10^{-30}

Table 7. Calculated total dipole moment μ (Debye), average polarizability α $(Å^3)$ for the compounds **1** and **2** using RB3LYP/6-31G(p, d).

Components	Compound **1**	Compound **2**
μ_x	−3.984	−2.660
μ_y	−2.601	0.572
μ_z	2.227	2.164
μ_{tot} (Debye)	5.253	3.477
α_x	331.793	317.27
α_y	245.409	232.987
α_z	157.993	155.843
$\bar{\alpha}$ $(Å^3)$	36.314	34.877

in compound **1** is greater than in compound **2**. This result is clearly due to the differences between these compounds, mostly due to the nature of the donor and acceptor groups attached to pyrrazolphthalazine entity.

Supplementary Information (SI)

Crystallographic information for compounds **1** and **2** have been deposited with the Cambridge crystallographic data center (CCDC): CCDC No. 1476722 and 1454729. The electronic Supplementary Information is available at www.ias.ac.in/chemsci.

Acknowledgements

We are grateful to the Ministère de l'Enseignement Supérieur et de la Recherche Scientifique—Algérie (MESRS) for financial support. AB thanks Professor H. Merazig (UR. CHEMS, Université des Frères Mentouri, Constantine) for his assistance in structural determination.

References

1. Xue D Q, Zhang X Y, Wang C J, Ma L Y, Zhu N, He P, Shao K P, Chen P J, Gu Y F, Zhang X S, Wang C F, Ji C H, Zhang QR and Liu H M 2014 Synthesis and anticancer activities of novel 1,2,4-triazolo[3,4-a]phthalazine derivatives *Eur. J. Med. Chem.* **85** 235
2. Zhang Q R, Xue D Q, He P, Shao K P, Chen P J, Gu Y F, Ren J L, Shan L H and Liu H M 2014 Synthesis and antimicrobial activities of novel 1,2,4-triazolo [3,4-a] phthalazine derivatives *Bioorg. Med. Chem. Lett.* **24** 1236
3. Ryu C K, Park R E, Ma M Y and Nho J H 2007 Synthesis and antifungal activity of 6-arylamino-phthalazine-5,8-diones and 6,7-bis(arylthio)-phthalazine-5,8-diones *Bioorg. Med. Chem. Lett.* **17** 2577
4. Sinkkonen J, Ovcharenko V, Zelenin K N, Bezhan I P, Chakchir B A, Al-Assar F and Pihlaja K 2002 ^{1}H]phthalazine-5,10-diones and Their Ring-Chain Tautomerism *Eur. J. Org. Chem.* **2002** 2046
5. Sangani C B, Makwana J A, Duan Y T, Thumar N J, Zhao M Y, Patel Y S and Zhu H L 2016 Synthesis of 1*H*-pyrazolo[1,2-b]phthalazine-5,10-dione derivatives: Assessment of their antimicrobial, antituberculosis and antioxidant activity *Res. Chem. Intermed.* **42** 2101
6. Watanabe N, Kabasawa Y, Takase Y, Matsukura M, Miyazaki K, Ishihara H, Kodama K and Adachi H 1998 4-Benzylamino-1-chloro-6-substituted phthalazines: Synthesis and inhibitory activity toward phosphodiesterase 5 *J. Med. Chem.* **41** 3367
7. Wu H, Chen X M, Wan Y, Xin H Q, Xu H H, Ma R, Yue C H and Pang L L 2009 Synthesis and Luminescence of 7-amino-2H-indazolo[2,1-b]phthalazine- 1,6,11(13H)-triones Catalyzed by Silica Sulfuric Acid *Lett. Org. Chem.* **6** 219
8. Prasad P N and Williams D J 1991 In *Introduction to nonlinear optical effects in molecules and Polymers* (New York: Wiley) pp. 120–131
9. Ekbote A, Patil P S, Maidur S R, Chia T S and Quah C K 2017 Structure and nonlinear optical properties of (E)-1-(4-aminophenyl)-3-(3-chlorophenyl) prop-2-en-1-one: A promising new D-π-D type chalcone derivative crystal for nonlinear optical devices *J. Mol. Struct.* **1129** 239
10. Morales A R, Frazer A, Woodward A W, Ahn-White H -Y, Fonari A, Tongwa P, Timofeeva T and Belfield K D 2013 Design, Synthesis, and Structural and Spectroscopic Studies of Push–Pull Two-Photon Absorbing Chromophores with Acceptor Groups of Varying Strength *J. Org. Chem.* **78** 1014
11. Ramkumar V, Anandhi S, Kannan P and Gopalakrishnan R 2013 Synthesis, single crystal growth, characterization and comparison of two new enone shifted chalcones and their NLO behavior *CrystEngComm***15** 2438
12. Arroudj S, Bouchouit M, Bouchouit K, Bouraiou A, Messaadia L, Kulyk B, Figa V, Bouacida S, Sofiani Z and Taboukhat S 2016 Synthesis, spectral, optical properties and theoretical calculations on schiff bases ligands containing o-tolidine *Opt. Mater.* **56** 116
13. Bouchouit M, Elkouari Y, Messaadia L, Bouraiou A, Arroudj S, Bouacida S, Taboukhat S and Bouchouit K 2016 Synthesis, spectral, theoretical calculations and optical properties performance of substituted-azobenzene dyes *Opt. Quant. Electron.* **48** 178
14. Nabid M R, Rezaei S J T, Ghahremanzadeh R and Bazgir A 2010 Ultrasound-assisted one-pot, three-component synthesis of 1H-pyrazolo[1,2-b]phthalazine-5,10-diones *Ultrason. Sonochem.* **17** 159
15. Safaei-Ghomi J, Shahbazi-Alavi H, Ziarati A, Teymuri R and Saberi M R 2014 A highly flexible green synthesis of 1H-pyrazolo[1,2-b]phthalazine-5,10-dione derivatives with CuI nanoparticles as catalyst under solvent-free conditions *Chin. Chem. Lett.* **25** 401
16. Khurana J M and Magoo D 2009 Efficient one-pot syntheses of 2H-indazolo[2,1-b] phthalazine-triones by catalytic H_2SO_4 in water–ethanol or ionic liquid *Tetrahedron Lett.* **50** 7300
17. Atar A B, Lee S D, Cho B G, Cho D W and Jeong Y T 2016 β: the most efficient catalyst for one-pot synthesis of 2H-indazolo[2,1-b]phthalazine-triones under solvent-free conditions *Res. Chem. Intermed.* **42** 1707
18. Burla M C, Caliandro R, Camalli M, Carrozzini B, Cascarano G L, De Caro L, Giacovazzo C, Polidori G and Spagna R 2005 an improved tool for crystal structure determination and refinement *J. Appl. Cryst.* **38** 381
19. Sheldrick G M 2008 A short history of SHELX *Acta Cryst. A* **64** 112
20. Farrugia L J 2012 WinGX and ORTEP for Windows: An update *J. Appl. Cryst.* **45** 849
21. Sheldrick G M 2002 SADABS Bruker AXS Inc., Madison, Wisconsin, USA
22. Maker D, Terhune R W, Niseno M F and Savage C M 1962 Effects of Dispersion and Focusing on the Production of Optical Harmonics *Phys. Rev. Lett.* **8** 21
23. Dennington R, Keith T and Millam J 2009 *GaussView* Version 5.0.9, Semichem Inc.: Shawnee Mission KS
24. Becke A D 1988 Density-functional exchange-energy approximation with correct asymptotic behavior *Phys. Rev. A* **38** 3098
25. Perdew J P 1986 Density-functional approximation for the correlation energy of the inhomogeneous electron gas *Phys. Rev. B* **33** 8822
26. Gubler U and Bosshard C 2000 Optical third-harmonic generation of fused silica in gas atmosphere: Absolute value of the third-order nonlinear optical susceptibility $\chi^{(3)}$ *Phys. Rev. B* **61** 10702
27. Kubodera K and Kobayashi H 1990 Determination of Third-Order Nonlinear Optical Susceptibilities for Organic Materials by Third-Harmonic Generation *Mol. Cryst. Liq. Cryst.* **182** 103

28. Fleming I 1976 *Frontier Orbitals and Organic Chemical Reactions* (New York: John Wiley) pp. 05–27
29. Zhang C R, Chen H S and Wang G H 2004 Structure and properties of semiconductor microclusters GanPn (n= 1-4): a first principle study *Chem. Res. Chin. U.* **20** 640
30. Sun Y, Chen X, Sun L, Guo X and Lu W 2003 Nanoring structure and optical properties of Ga_8As_8 *Chem. Phys. Lett*. 397
31. Kleinman, D A 1962 Nonlinear Dielectric Polarization in optical media *Phys. Rev.* **126** 1977